

ARTICLE

Received 13 Oct 2016 | Accepted 20 Apr 2017 | Published 30 May 2017

DOI: 10.1038/ncomms15686

OPEN

Coral calcification in a changing World and the interactive dynamics of pH and DIC upregulation

Malcolm T. McCulloch^{1,2}, Juan Pablo D'Olive^{1,2}, James Falter^{1,2}, Michael Holcomb^{1,2} & Julie A. Trotter¹

Coral calcification is dependent on the mutualistic partnership between endosymbiotic zooxanthellae and the coral host. Here, using newly developed geochemical proxies ($\delta^{11}\text{B}$ and B/Ca), we show that *Porites* corals from natural reef environments exhibit a close ($r^2 \sim 0.9$) antithetic relationship between dissolved inorganic carbon (DIC) and pH of the corals' calcifying fluid (cf). The highest DIC_{cf} ($\sim \times 3.2$ seawater) is found during summer, consistent with thermal/light enhancement of metabolically (zooxanthellae) derived carbon, while the highest pH_{cf} (~ 8.5) occurs in winter during periods of low DIC_{cf} ($\sim \times 2$ seawater). These opposing changes in DIC_{cf} and pH_{cf} are shown to maintain oversaturated but stable levels of carbonate saturation ($\Omega_{\text{cf}} \sim \times 5$ seawater), the key parameter controlling coral calcification. These findings are in marked contrast to artificial experiments and show that pH_{cf} upregulation occurs largely independent of changes in seawater carbonate chemistry, and hence ocean acidification, but is highly vulnerable to thermally induced stress from global warming.

¹Oceans Institute and School of Earth Sciences, The University of Western Australia, Crawley, Western Australia 6009, Australia. ²ARC Centre of Excellence for Coral Reef Studies, The University of Western Australia, Crawley, Western Australia 6009, Australia. Correspondence and requests for materials should be addressed to M.T.M. (email: malcolm.mcculloch@uwa.edu.au).

Scleractinian corals together with their endosymbiotic dinoflagellates, *Symbiodinium* (zooxanthellae), have been spectacularly successful in building the tropical coral reef edifices that dominate many shallow-water environments and harbour more than one-third of the oceans' biodiversity. The ongoing viability of these iconic¹ tropical reef systems is however in question^{2,3}, with symbiont-bearing shallow-water corals now facing the combined challenge of both global warming and ocean acidification from rapidly rising levels of CO₂ (ref. 4). Critical to the success of reef-building corals is their ability to extract dissolved inorganic carbon (DIC) from seawater and efficiently convert it into calcium carbonate, the major constituent of their skeletons. While much progress has been made in identifying many of the key elements of the biologic machinery that are integral to the biocalcification process^{5–7} (Fig. 1), there are still significant gaps in our understanding. Foremost is the relationship between declining seawater pH and its impact on pH upregulation of the coral's extracellular calcifying fluid^{8–10}, a process that occurs at least in part via Ca-ATPase pumping of Ca²⁺ ions into the calcifying region in exchange for the removal of protons¹¹. Of equal but largely overlooked importance, are the mechanisms via which the various pH-dependent species of DIC (that is, CO₂, HCO₃⁻ or CO₃²⁻) are produced, transported, and then inter-converted at the site of calcification. It has also long been recognized^{12,13} that light plays a key role in driving rates of calcification, and that light-enhanced calcification occurs as a result of the photosynthetic activity of endosymbiotic dinoflagellates (zooxanthellae), providing both energy and additional carbon needed to drive calcification. The exact mechanism(s) by which coral calcification is linked to endosymbiont photosynthesis has, however, remained largely enigmatic at the polyp scale (Fig. 1) the zooxanthellae are physically separated from the site of calcification^{13–15} and, apart from pH, few direct measurements exist¹⁶ of the chemical conditions necessary to constrain the biocalcification process. Here we provide new evidence for an intimate link between the biologically mediated process of pH_{cf} upregulation of the calcifying fluid and biological control over the concentration of DIC in the calcifying fluid (DIC_{cf}). We find that over annual timescales there is an inverse correlation between pH_{cf} and DIC_{cf}. This acts to maintain relatively stable levels of aragonite saturation in the calcifying fluid, and hence near-optimal rates of coral calcification, despite large seasonally driven variations in metabolically supplied DIC.

Results

Reef-water and coral calcifying fluid carbonate chemistry. To reconstruct the carbonate chemistry of the calcifying fluid from which corals precipitate their aragonite skeleton, we use the boron isotopic composition (δ¹¹B) as a proxy for the calcifying fluid pH_{cf} (refs 10,17,18). For determining the carbonate ion concentrations [CO₃²⁻]_{cf} in the calcifying fluid, we use the combined δ¹¹B-B/Ca proxy¹⁹. The application of the δ¹¹B-B/Ca carbonate ion proxy has now been made possible by recent experimental measurements of the B/Ca carbonate ion distribution coefficient¹⁹, a major limitation of previous studies²⁰ (see 'Methods' section). To examine how the chemistry of the calcifying fluid varies seasonally under 'real-world' reef conditions, we have analysed the skeletons of massive *Porites* collected from Davies Reef in the Great Barrier Reef and from Coral Bay Ningaloo Reef for which reef-water pH and sea-surface temperatures (SST) records are available^{21,22} (see 'Methods' section). Species of massive *Porites* coral are ideal for reconstructing seasonal changes in the composition of their calcifying fluid since they are long-lived and, more importantly,

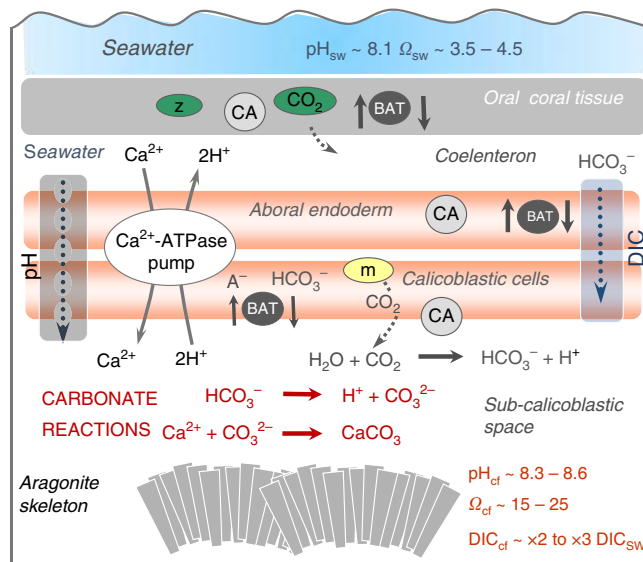


Figure 1 | Mechanisms involved in coral calcification. Calcification occurs within the subcalicoblastic space from an initial seawater-derived fluid with additional metabolic sourced supply of DIC^{5–7}. Elevation of calcifying fluid pH_{cf} occurs via removal of protons from the calcification site by Ca²⁺-ATPase exchangers. The carbonic anhydrases (CA) catalyse the forward reactions converting CO₂ into HCO₃⁻ ions^{7,34}. Transfer of DIC into the subcalicoblastic space may occur via diffusion of CO₂ and/or by HCO₃⁻ pumping via bicarbonate anion transporters (BAT)^{5–7}. The link between the activity of zooxanthellae located in the oral coral endoderm tissue to the generation of metabolic DIC within the aboral endoderm and calcicoblastic cells (orange) and transport to the calcifying fluid remains uncertain^{5–7} (Figure modified from McCulloch *et al.*³¹).

the architecture of their skeleton has a relatively straightforward chronology that facilitates well-constrained timing of their skeletal growth at seasonal resolution²³. Given that only limited records of seasonal changes in local seawater carbonate chemistry are available^{22,24}, these data are supplemented by model estimates²⁴ of the reef-induced pH variability. The Great Barrier Reef and Ningaloo Reef sites (see 'Methods' section) have a typical seasonal range in temperature from ~23 to 28 °C, as well as relatively narrow seasonal ranges in seawater pH_{sw} (total scale) from ~8.02 in summer to ~8.08 in winter (Fig. 2). This limited seasonal range in average reef-water pH_{sw} of ~0.06 pH units is comparable to that observed in the open ocean²⁵, a reflection of the tight balance between production and respiration²⁴ combined with the limited residence time of waters in most wave and tidally driven reef systems²¹.

Covariation of calcifying fluid pH_{cf} and DIC_{cf}. In contrast to the limited variation in reef-water pH_{sw}, we find that *Porites* colonies from both Davies Reef and Coral Bay exhibit strong seasonal changes in pH_{cf} from ~8.3 during summer to ~8.5 during winter (Fig. 2). This represents an elevation in pH_{cf} relative to ambient seawater of ~0.4 pH units together with a relatively large seasonal range in pH_{cf} of ~0.2 units. These observations are in stark contrast to the far more muted changes based on laboratory-controlled experiments^{9,17}. These inferred laboratory responses¹⁰ in calcifying fluid pH (pH_{cf}^{*}) are shown in Figs 2 and 4, where the expected seasonal range is ~0.02 pH units, an order of magnitude smaller than those actually observed in reef environments. The explanation for this unexpectedly large range in seasonal pH_{cf} present under natural reef conditions becomes apparent from the exceptionally strong and inverse

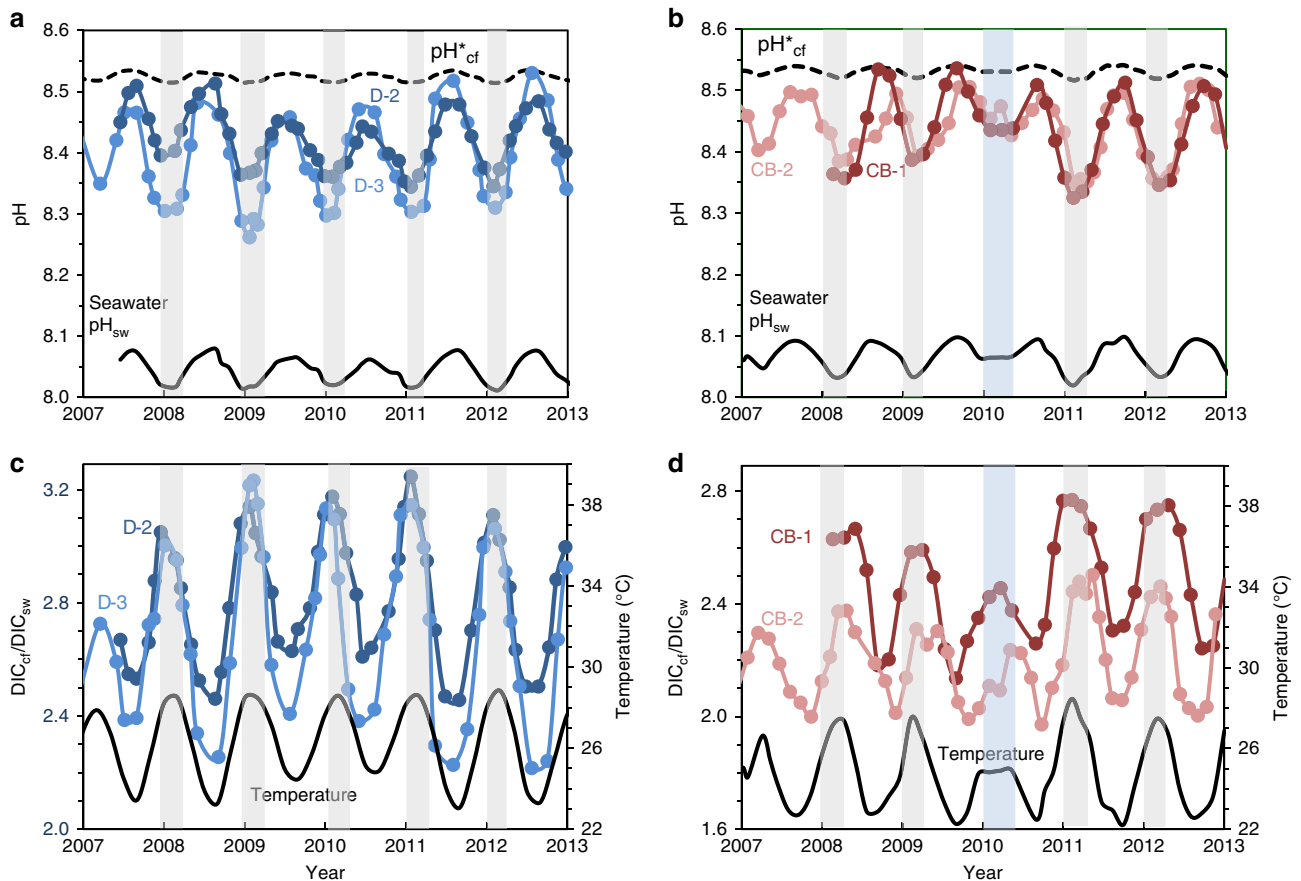


Figure 2 | Seasonal time series of coral calcifying fluid pH_{cf} and DIC_{cf} . (a) *Porites* spp. coral calcifying fluid pH_{cf} derived from $\delta^{11}\text{B}$ systematics (see ‘Methods’ section and Supplementary Data) for colonies D-2 and D-3 from Davies Reef (18.8°S) in the Great Barrier Reef, Queensland. Shading denotes the summer period when pH_{cf} and seawater pH_{sw} values are at a minimum. Dashed line shows pH_{cf}^* expected from artificial experimental calibrations ($\text{pH}_{\text{cf}}^* = 0.32 \text{pH}_{\text{sw}} + 5.2$)^{10,17} with an order of magnitude lower seasonal range than measured pH_{cf} values. (b) Same as previous for *Porites* colonies from Coral Bay (CB-1 and CB-2) in the Ningaloo Reef of Western Australia (23.2°S) showing seasonal fluctuations in pH_{cf} and seawater pH_{sw} . The blue shading denotes the anomalously cool summer temperatures in 2010. (c) Enrichments in calcifying fluid DIC_{cf} (left axis; coloured circles) derived from combined B/Ca and $\delta^{11}\text{B}$ systematics together with synchronous seasonal variations in reef-water temperatures (right axis; black line) for *Porites* colonies from Davies Reef (GBR). The strong temperature/light control on DIC_{cf} is consistent with enhanced metabolic activity of zooxanthellae symbionts in summer. (d) Same as previous but for *Porites* from Coral Bay (Ningaloo Reef, Western Australia).

correlations between pH_{cf} and DIC_{cf} ($r^2 = 0.88\text{--}0.94$) present at the colony level (Fig. 3a,b).

Here DIC_{cf} reaches its highest values in summer ($\times 2.0$ to $\times 3.2$ higher than ambient seawater) and lowest values in winter, whereas pH_{cf} shows the opposite pattern. This seasonal variability in DIC_{cf} is consistent with light- and temperature-driven changes in the supply of metabolic DIC provided by the endosymbionts and/or the bicarbonate anion transporters within the coral host⁷. Thus, each *Porites* colony forms a distinctive subparallel array characterized by a distinctive range in DIC_{cf} that is inversely correlated to pH_{cf} . Since the concentrations of carbonate ion [CO_3^{2-}] and consequently the aragonite saturation state ($\Omega_{\text{cf}} = [\text{Ca}^{2+}]_{\text{cf}} [\text{CO}_3^{2-}]_{\text{cf}} / K_{\text{arag}}$) of the calcifying fluid increases with increasing DIC_{cf} and pH_{cf} , the observed antithetic seasonal changes in these parameters results in a more muted seasonal variation in Ω_{cf} ($\pm 5\%$ to $\pm 10\%$, Fig. 3a) compared to that expected from changes in only pH_{cf} ($\pm 30\%$) or DIC_{cf} ($\pm 12\%$) acting alone. While there remains a subdued positive correlation of Ω_{cf} with temperature (Fig. 3a), the inverse correlations between pH_{cf} and DIC_{cf} (Fig. 2a,b) indicate that the coral is actively maintaining both high ($\sim \times 4$ to $\times 6$ seawater) and relatively stable (within $\pm 10\%$ of mean) levels of elevated Ω_{cf} year-round.

While the absolute levels of enhanced Ω_{cf} are not dissimilar to previous qualitative estimates^{17,26}, the finding of significantly higher but relatively limited ranges in DIC_{cf} of $\sim \times 2.0$ to $\sim \times 3.2$ seawater, is not generally consistent with recent micro-sensor¹⁶ measurements. This difference may reflect the intrinsic limitations⁶ of using probes that are $15\text{--}20\ \mu\text{m}$ wide to measure the chemistry within the much narrower and irregular ($1\text{--}10\ \mu\text{m}$) calcifying region. Additionally, separate probes are required for measurements of pH_{cf} and [CO_3^{2-}]_{cf}, introducing further uncertainty, likely accounting for the large variability of *in situ* measured CO_3^{2-} and hence inferred DIC_{cf} ($\sim \times 1.4$ to $\times 4.2$ seawater). Finally and most importantly, regardless of the method employed, we find that measurements conducted under controlled, static, laboratory conditions¹⁰ are unlikely to be representative of natural reef conditions due to the interactive dynamics of pH_{cf} and DIC_{cf} upregulation described herein.

Discussion

The underlying reason for the dynamic, antiphase relationship between pH_{cf} versus DIC_{cf} can be explained by the ability of the coral to ‘control’ what is arguably²⁷ one of its most fundamental

physiological processes, the growth of its skeleton within which it lives. For example, during winter (Fig. 2), there is a large systematic decrease in the abundance of metabolic DIC ($\sim 25\%$), presumably as a consequence of reductions in both light and temperature. Since higher pH shifts the carbonate equilibria to favour CO_3^{2-} relative to HCO_3^- , the greater increase in pH_{cf} in winter (~ 8.5) compared to summer (~ 8.3) increases the concentration of carbonate ions within the calcifying fluid (and therefore Ω_{cf}) for the same DIC_{cf} . This increase in winter pH_{cf} therefore partially counters the seasonal slowdown in host-symbiont carbon metabolism. Hence during the cooler periods, higher pH_{cf} enhances Ω_{cf} and hence partially mitigates the reduced temperature-dependent kinetics of calcification because rates of mineral precipitation are proportional to $(\Omega - 1)^n$, where n is the temperature-dependent order of the reaction²⁸ ($n = 1.3\text{--}2.0$ for most reef habitats). During summer, the opposite behaviour is observed, with higher rates of metabolic DIC_{cf} partially offset by decreases in pH_{cf} , resulting in a concomitant decrease in the carbonate saturation state of the calcifying fluid (Ω_{cf}) and hence moderated (albeit still high) rates of calcification (Fig. 4c,d).

This implies that during summer, zooxanthellae-derived DIC_{cf} is being supplied in excess of the 'optimal' requirements for the biologically mediated process of skeleton building. Thus, while existing mineral rate kinetics indicate that rates of calcification are still a factor of two- to fourfold higher in summer than in winter, this range is significantly less than the estimated eightfold higher summer rates (Fig. 4c,d) if constant levels of elevated pH_{cf} upregulation were operative, as implied from the artificial constant seawater pH_{sw} and temperature experiments¹⁰.

Although our findings are based only on species of *Porites* from the Pacific and Indian Oceans, they nevertheless have important implications for our understanding of how reef-building corals in general will respond to climate change. The occurrence, for example, of the highest pH_{cf} values during winter, when metabolically derived sources of energy are at a minimum, provides further evidence against the proposition that pH_{cf} upregulation is an energetically costly process²⁹, and will therefore decline as seawater pH_{sw} decreases due to ocean acidification. This is supported by results of the free ocean carbon enrichment experiment³⁰ conducted within the GBR Heron Island lagoon, where corals subjected to both natural and superimposed fluctuations in seawater pH_{sw} exhibited essentially constant pH_{cf} upregulation, a condition referred to by those authors³⁰ as 'pH homeostasis'. These findings, combined with measurements of even higher pH_{cf} in azooxanthellate deep-sea corals³¹ ($\text{pH}_{\text{cf}} > 8.6$), are thus consistent with inferences that Ca-ATPase-driven pH_{cf} upregulation is a relatively energetically inexpensive process¹⁷. These observations, in conjunction with the highly correlated and anti-cyclical seasonal changes in both pH_{cf} and DIC_{cf} , therefore argue against the reduction of pH_{cf} in summer being a result of the passive feedback from higher rates of calcification producing more protons thereby lowering pH_{cf} . Thus, while this possibility cannot yet be entirely excluded, the higher production rates of zooxanthellae-derived metabolites that are presumably available in the summer to facilitate enhanced Ca-ATPase activity, also suggest that the lower summer levels of pH_{cf} is not due to intrinsic limitations in the Ca-ATPase H^+ pumping, but rather physiological controls on growth rate. Furthermore, similar anti-correlated changes in pH_{cf} and DIC_{cf} are present in *Porites* from both Davies and Ningaloo Reefs, despite large differences in growth rates.

Our findings also have major ramifications for the interpretation of the large number of experiments that have reported a strong sensitivity of coral calcification to increasing

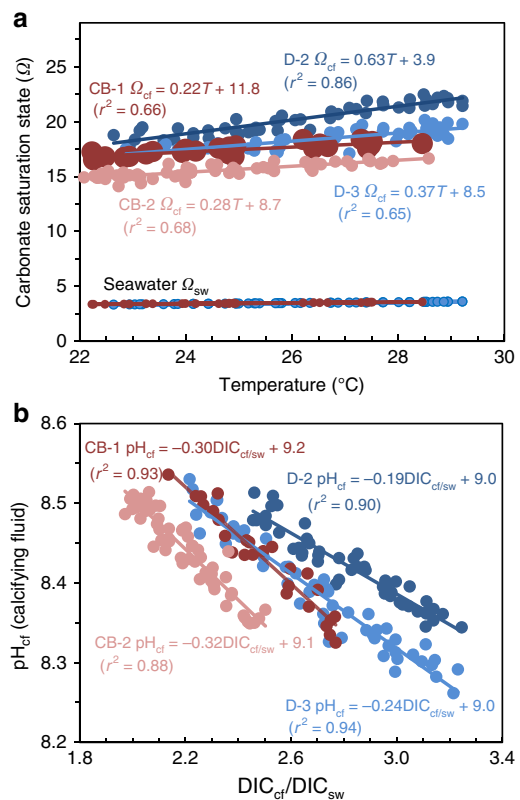


Figure 3 | Covariation between calcifying fluid parameters Ω_{cf} versus seasonal temperature and pH_{cf} versus DIC_{cf} . (a) Covariation of calcifying fluid saturation state (Ω_{cf}) with reef-water temperature showing a five- to sixfold elevation in Ω_{cf} relative to reef-waters for *Porites* corals from Davies Reef (D-2 and D-3) in the Great Barrier Reef and from Coral Bay (CB-1 and CB-2) in the Ningaloo Reef. Note the very narrow range (± 5 to $\pm 10\%$) of high Ω_{cf} values for each colony. (b) Subparallel arrays of inversely correlated ($r^2 = 0.88\text{--}0.94$) calcifying fluid pH_{cf} and $\text{DIC}_{\text{cf}}/\text{DIC}_{\text{sw}}$ values reflecting specific bio-environmental controls at the colony level on metabolic $\text{DIC}_{\text{cf}}/\text{DIC}_{\text{sw}}$. Seasonal variations in metabolic supplied DIC_{cf} are offset by opposing changes in pH_{cf} that act to moderate the overall variations in Ω_{cf} , the ultimate controller of skeletal growth rates.

ocean acidification³². An inherent limitation of many of these experiments³³ is that they were generally conducted under conditions of fixed seawater pH_{sw} and/or temperature, light, nutrients, and little water motion, hence conditions that are not conducive to reproducing the natural interactive effects between pH_{cf} and DIC_{cf} that we have documented here. A characteristic common to a variety of coral species grown under these artificial conditions is the apparently constant but limited sensitivity (one-third to one-half) of pH_{cf} relative to external changes in seawater pH_{sw} (refs 10,17). While the reason for this apparently systematic but muted experimental response of pH_{cf} is still uncertain, it likely involves reduced and/or constant levels of metabolically produced DIC_{cf} . Under such fixed conditions, we surmise that the supply of seawater DIC into the subcalicoblastic space (Fig. 1) becomes the dominant source and hence major influence on levels of DIC_{cf} , with upregulation of pH_{cf} therefore acting as the major controller of Ω_{cf} and thereby affecting the perceived sensitivity of pH_{cf} to ocean acidification. This inference is supported by the fact that the observed pH_{cf} of *Porites* from both Davies and Ningaloo Reefs were closest to the pH_{cf} predicted from the constant condition experiments in winter when DIC_{cf} levels are naturally lowest due to reduced light and/or temperature, hence most similar to experimental predicted

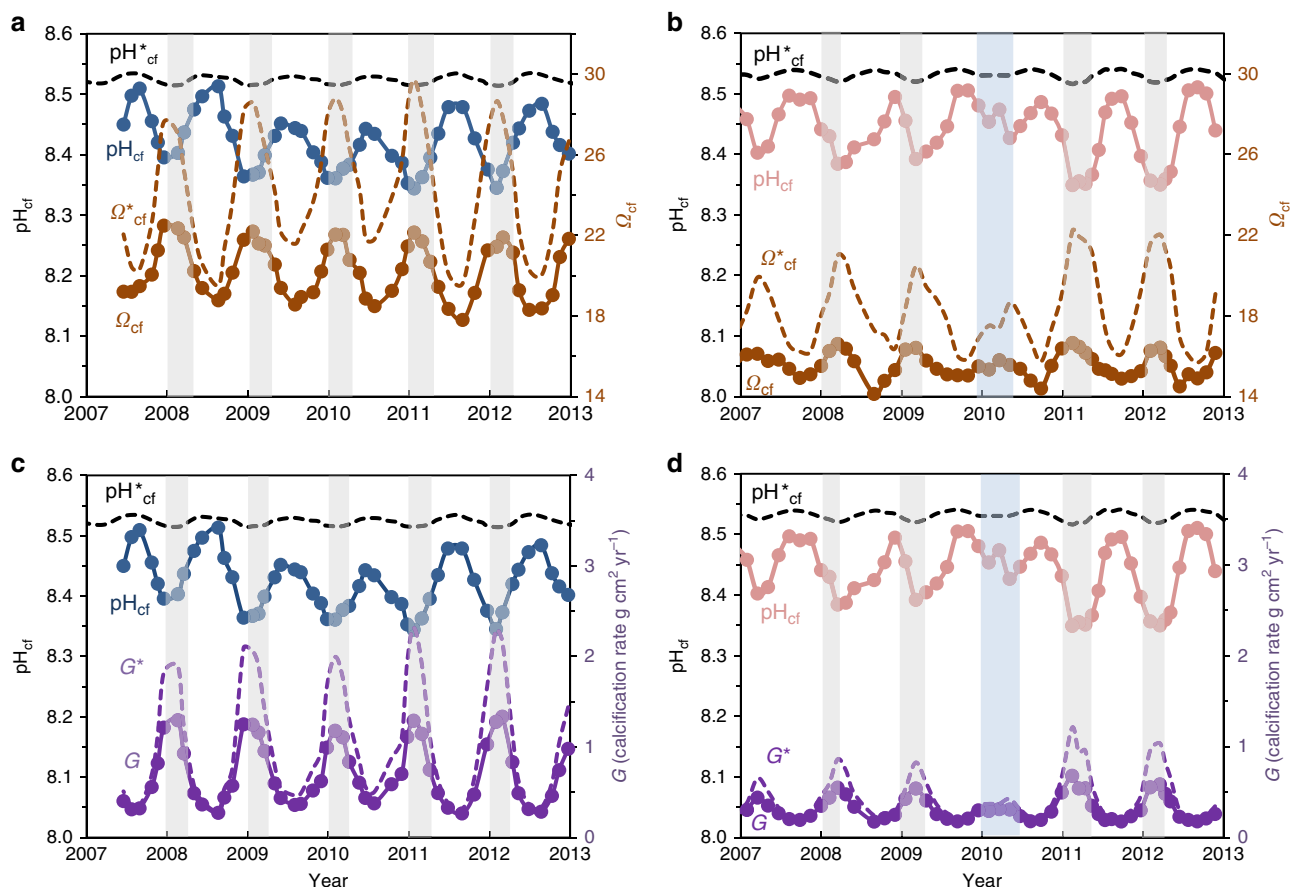


Figure 4 | Seasonal time series of calcifying fluid pH_{cf} and Ω_{cf} together with calculated calcification rates G . (a) Calcifying fluid pH_{cf} and Ω_{cf} values for *Porites* coral (D-2) from Davies Reef (GBR), where $\Omega_{\text{cf}} = [\text{Ca}^{2+}]_{\text{cf}} [\text{CO}_3^{2-}]_{\text{cf}} / K_{\text{arag}}$. Dashed line shows the Ω_{cf}^* calculated using fixed experimental^{10,17} pH_{cf}^* values (see Fig. 2a,b). (b) Same as previous for Coral Bay (Ningaloo Reef, Western Australia) *Porites* (CB-2). (c) Calcification rates calculated using the inorganic rate equation²⁸ $G = k(\Omega - 1)^n$, where k and n are the temperature-dependent constant and order of the reaction, respectively²⁸. Because of opposing changes in pH_{cf} relative to DIC_{cf} (Fig. 1), Ω_{cf} and hence coral growth rates are strongly modulated reducing seasonal variations by twofold compared to those estimated from fixed condition experiments (G^*). (d) Same as previous for *Porites* from Coral Bay (Ningaloo Reef, Western Australia).

seawater end-member values. Clearly, since the interactive dynamics of pH_{cf} and DIC_{cf} upregulation do not appear to be properly simulated under the short-term conditions generally imposed by such artificial experiments, the relevance of their commonly reported finding of reduced coral calcification with reduced seawater pH must now be questioned.

In summary, we have now identified the key functional characteristics of chemically controlled calcification in reef-building coral. The seasonally varying supply of summer-enhanced metabolic DIC_{cf} is accompanied by dynamic out-of-phase upregulation of coral pH_{cf} . These parameters acting together maintain elevated but near-constant levels of carbonate saturation state (Ω_{cf}) of the coral's calcifying fluid, the key driver of calcification. Although the maintenance of elevated but near-constant Ω_{cf} in mature coral colonies is not directly influenced by ocean acidification, it is however highly susceptible to thermal stress. In extreme cases of coral bleaching, the loss of endosymbionts disrupts the metabolic supply of DIC_{cf} as well as the metabolites necessary to operate the Ca-ATPase that upregulate pH_{cf} (refs 14,34), thus effectively terminating calcification. So, although rising levels of p_{CO_2} can have adverse effects on the recruitment and growth of juvenile corals^{35–38}, especially those lacking robust internal carbonate chemistry regulatory mechanisms, extreme thermal stress is detrimental to all symbiont-bearing corals^{39,40} regardless of their growth stage.

We therefore conclude that the increasing frequency and intensity of coral bleaching events due to CO_2 -driven global warming constitutes the greatest immediate threat to the growth of shallow-water reef-building corals, rather than the closely associated process of ocean acidification.

Methods

Reef sites. *Porites* colonies were sampled from two reef systems: (1) Davies Reef (18.8° S, 147.63° E), a mid-shelf reef ~100 km east-northeast of Townsville, Queensland, Australia in the central Great Barrier Reef, and (2) Coral Bay (23.19° S, 113.77° E), part of the Ningaloo Reef coastal fringing system of Western Australia. At Davies Reef, the annual range of daily average SST is 23–28.5 °C with a diurnal range of ~0.5 °C or less⁴¹. *In situ* seawater temperature data extending back to 1987 for the core site at Davies Reef (18.83° S, 147.63° E) was compiled from a number of different temperature sensors deployed between a depth of ~2 to ~10 m maintained by the Australian Institute of Marine Science from October 1991 to December 2013 (<http://data.aims.gov.au/aimstrds/datatool.xhtml>). To estimate seasonal changes in carbonate chemistry, we used the 24-h seawater carbonate chemistry data collected by Albright *et al.*²² on the lagoon side of the Davies Reef flat around the summer and winter extremes in both light and temperature. Their data showed that the daily average pH at that reef site was 8.02 in summer and 8.08 in winter; a seasonal range that was similar to seasonal minima and maxima observed and hind-cast at Coral Bay and hence similar to what would be expected from seasonal variations in temperature-driven p_{CO_2} solubility. We therefore assumed that daily average pH at Davies Reef also followed seasonal changes in temperature according to $\text{pH}_{\text{sw}} = -0.010 \times T + 8.31$.

At Coral Bay, SST generally ranges from 22–23 °C in winter to 27–28 °C in summer²¹. To hind-cast seasonal changes in reef-water temperature and pH, we first used time series of SST data from just offshore Coral Bay at ~25 km

resolution produced by Reynolds *et al.*⁴² before June 2010 and then at ~ 1 km resolution produced by Chao *et al.*⁴³ Both SST data products were then calibrated against *in situ* observations of temperature collected from a moored depth of ~ 17 m as described by Falter *et al.*²¹ and previous model studies of wave-driven circulation. The carbonate chemistry of Coral Bay and offshore waters (~ 2 km) were monitored between May 2011 and June 2012 and intermittently since then, with seasonal changes in offshore seawater pH_T (total scale) being found to be strongly correlated with seasonal changes in offshore temperature ($\text{pH}_{\text{sw}} = -0.012 \times T + 8.37$, $r^2 = 0.86$, $n = 13$). To determine seasonal changes in pH at the back-reef site where the coral cores were recovered, the offshore pH was adjusted to account for the deviation in temperature due to local heating and cooling (see above), as well as the daily average decrease in total alkalinity of $\sim 10 \mu\text{mol kg}^{-1}$ at back-reef sites observed from measurements⁴⁴.

Boron isotopic pH proxy. Changes in the isotopic ratio of ^{11}B ($\sim 80\%$) and ^{10}B ($\sim 20\%$) are expressed in delta notation (in per mil, ‰) as:

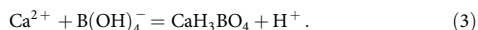
$$\delta^{11}\text{B}_{\text{carb}} = \left[\left(\frac{^{11}\text{B}/^{10}\text{B}_{\text{carb}}}{^{11}\text{B}/^{10}\text{B}_{\text{NIST951}}} \right) - 1 \right] \times 1,000, \quad (1)$$

where $^{11}\text{B}/^{10}\text{B}_{\text{carb}}$ is the isotopic ratio measured in the coral carbonate and $^{11}\text{B}/^{10}\text{B}_{\text{NIST951}}$ is the isotopic ratio of the NIST SRM 951 boric acid standard. In seawater, boron exists as two different species, boric acid ($\text{B}(\text{OH})_3$) and the borate ion ($\text{B}(\text{OH})_4^-$), with their relative abundance being pH dependent. The sensitivity of the $\delta^{11}\text{B}$ proxy to the calcifying fluid pH_{cf} arises from the incorporation of only the borate ion species into the aragonite structure^{45–47}, with the $\delta^{11}\text{B}$ isotopic composition reflecting the pH sensitivity of the borate versus boric acid speciation. The pH of the calcifying fluid (pH_{cf}) can thus be calculated from the $\delta^{11}\text{B}$ measured in the coral carbonate ($\delta^{11}\text{B}_{\text{carb}}$). The equation used to convert the $\delta^{11}\text{B}_{\text{carb}}$ isotopic composition measured in the coral carbonate skeleton to a pH of the calcifying fluid (pH_{cf}) is given by⁴⁸:

$$\text{pH}_{\text{cf}} = \text{p}K_{\text{B}} - \log \left[\frac{(\delta^{11}\text{B}_{\text{sw}} - \delta^{11}\text{B}_{\text{carb}})}{(\alpha_{(\text{B}3-\text{B}4)} \delta^{11}\text{B}_{\text{carb}} - \delta^{11}\text{B}_{\text{sw}} + 1,000(\alpha_{(\text{B}3-\text{B}4)} - 1))} \right], \quad (2)$$

where $\delta^{11}\text{B}_{\text{sw}}$ represents the $\delta^{11}\text{B}$ in seawater ($\delta^{11}\text{B}_{\text{sw}} = 39.61\%$)⁴⁹ and $\alpha_{(\text{B}3-\text{B}4)} = 1.0272$ (ref. 50). The dissociation constant of boric acid $\text{p}K_{\text{B}}$ has a well-established value of 8.597 at 25 °C and a salinity of 35 (ref. 51). Here we also assume that the calcifying fluid has the same $\delta^{11}\text{B}$ composition as seawater since that is the ultimate source of boron and, due to the low K_{D} of B/Ca (ref. 19), the boron composition and concentration of the calcifying fluid remains essentially constant during calcification. Recent studies utilizing the $\delta^{11}\text{B}$ pH_{cf} proxy as well as direct measurements of calcifying fluid pH using pH-sensitive dyes^{9,18}, have also confirmed that under highly controlled artificial conditions of constant pH and temperature, corals upregulate the pH_{cf} of their calcifying fluid by $1/3$ to $1/2$ relative to ambient seawater pH.

B/Ca constraints on calcifying fluid DIC concentrations. Prior studies indicate that borate rather than boric acid is the predominant species occupying the lattice position normally taken up by the carbonate ion⁵² in calcifiers that precipitate aragonite skeletons. Although there are a number of reaction pathways through which this substitution could occur^{19,20}, it is likely to involve de-protonation of the borate species to create a divalent base ion with the same charge as that of the carbonate ion species (-2), to preserve the charge neutrality of the growing crystal:



The partitioning of borate versus carbonate into aragonite is thus likely to be sensitive to solution pH^{10,19,20}. Here the relevant partition coefficient K_{D} relating the molar ratio of $(\text{B}/\text{Ca})_{\text{CaCO}_3}$ to the concentrations of the carbonate $[\text{CO}_3^{2-}]_{\text{sol}}$ and borate $[\text{B}(\text{OH})_4^-]_{\text{sol}}$ species in the precipitating solution is determined using:

$$K_{\text{D}} \equiv (\text{B}/\text{Ca})_{\text{CaCO}_3} \times \frac{[\text{CO}_3^{2-}]_{\text{sol}}}{[\text{B}(\text{OH})_4^-]_{\text{sol}}}. \quad (4)$$

Holcomb *et al.*¹⁹ conducted experiments quantifying the ratio of boron to calcium in aragonite precipitated inorganically under a wide range of carbonate chemistries (including pH) and total DIC and boron concentrations, as well as conditions of pH and DIC appropriate to those in the calcifying fluid of corals. Furthermore, Holcomb *et al.*¹⁹ also showed the close relationships between B/Ca, CO_3^{2-} and K_{D} based on substitution reactions between $\text{B}(\text{OH})_4^-$ and CO_3^{2-} . Re-analysing the Holcomb *et al.*¹⁹ data, we find (Fig. 5) that the observed K_{D} as defined in equation (4) shows the expected decrease as a function of the concentration of total active protons within the precipitating solution.

Thus, using the definition of K_{D} from equation (4) and its dependency on pH_{cf} as given by the inorganic data of Holcomb *et al.*¹⁹, we can now calculate the concentration of carbonate ions within the calcifying fluid (that is, $[\text{CO}_3^{2-}]_{\text{cf}}$ from measurements of $(\text{B}/\text{Ca})_{\text{carb}}$ and pH_{cf} , the latter derived from the skeletal boron isotopic ratio ($\delta^{11}\text{B}_{\text{carb}}$). We further assume that $[\text{B}_T]_{\text{cf}}$ is equal to the total concentration of boron of ambient seawater and only a function of seawater salinity

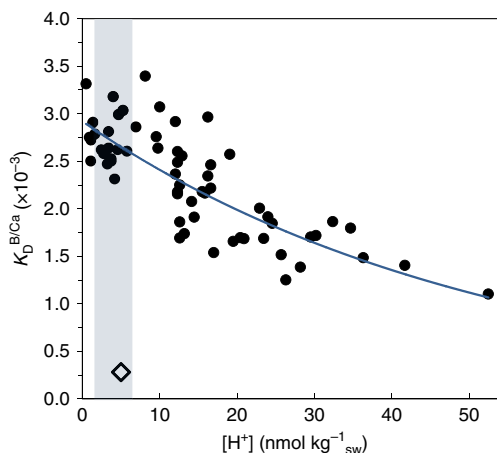


Figure 5 | Experimentally determined B/Ca partition coefficient as a function of hydrogen ion concentration. Measured B/Ca partition coefficient (K_{D}) as defined by equation (4) from the data of Holcomb *et al.*¹⁹ The line represents a best-fit exponential curve to the data with $K_{\text{D}}^{\text{B}/\text{Ca}} = K_{\text{D},0} \exp(-k_{\text{K}_0} [\text{H}^+]_{\text{T}})$, where $K_{\text{D},0} = 2.97 \pm 0.17 \times 10^{-3}$ ($\pm 95\%$ CI), $-k_{\text{K}_0} = 0.0202 \pm 0.042$, $r^2 = 0.64$ and $n = 63$. The range for pH_{cf} of upregulating calcifiers (that is, *Porites* spp.) is between ~ 8 and ~ 9 (shaded); equivalent to $[\text{H}^+]_{\text{T}}$ of between 1 and 10 nmol kg^{-1} giving a range in $K_{\text{D}}^{\text{B}/\text{Ca}}$ ($\times 10^{-3}$) of 2.6–2.8, and therefore relatively in-sensitive to changes in coral pH_{cf} . Importantly, our experimentally determined $K_{\text{D}}^{\text{B}/\text{Ca}}$ value is an order of magnitude higher than the previous estimate by Allison *et al.*²⁰ (open diamond) and consistent with the substitution of $\text{B}(\text{OH})_4^-$ with CO_3^{2-} .

($[\text{B}_T]_{\text{cf}} = [\text{B}_T]_{\text{sw}}$ at salinity = 35). We therefore have:

$$[\text{CO}_3^{2-}]_{\text{cf}} = K_{\text{D}} \times [\text{B}(\text{OH})_4^-]_{\text{cf}} / (\text{B}/\text{Ca})_{\text{CaCO}_3} \quad (5)$$

Where $K_{\text{D}} = 0.00297 \exp(-0.0202 [\text{H}^+]_{\text{T}})$ and for typical calcifying fluid pH_{cf} values $K_{\text{D}} \sim 0.0027$, an order of magnitude higher than a previous estimate²⁰. The concentration of DIC within the calcifying fluid is then calculated from the measured pH_{cf} (equation 1) and $[\text{CO}_3^{2-}]_{\text{cf}}$ (equation 2) values using the programme CO_2SYS provided by Lewis and Wallace⁵³, with the carbonate species dissociation constants of Mehrbach *et al.*⁵⁴ as re-fitted by Dickson and Millero⁵⁵, the borate and sulfate dissociation constants of Dickson^{51,56}, and the aragonite solubility constants of Mucci⁵⁷. We also note that our use of a reliable experimentally determined K_{D} is now consistent with substitution of borate with carbonate ion, rather than the previously inferred²⁰ substitution with bicarbonate ion, the latter assumption effectively negating the role of carbonate saturation state on calcification.

Data availability. The coral geochemical and seawater carbonate chemistry and temperature data are available in Supplementary Data.

References

1. Darwin, C. *The Voyage of the Beagle: Journal of Researches into the Natural History and Geology of the Countries Visited During the Voyage of HMS Beagle Round the World* (Modern Library, 2010).
2. Hughes, T. P. *et al.* Climate change, human impacts, and the resilience of coral reefs. *Science* **301**, 929–933 (2003).
3. Hoegh-Guldberg, O. Climate change, coral bleaching and the future of the world's coral reefs. *Mar. Freshw. Res.* **50**, 839–866 (1999).
4. Ciais, P. *et al.* in *Climate Change 2013: The Physical Science Basis. Contribution of Working Group I to the Fifth Assessment Report of the Intergovernmental Panel on Climate Change* (eds Stocker, T. F. *et al.*) 465–570 (Cambridge University Press, 2014).
5. Furla, P., Galgani, I., Durand, I. & Allemand, D. Sources and mechanisms of inorganic carbon transport for coral calcification and photosynthesis. *J. Exp. Biol.* **203**, 3445–3457 (2000).
6. Allemand, D., Tambutté, E., Zoccola, D. & Tambutté, S. in *Coral Reefs: An Ecosystem In Transition* Vol. III (eds Dubinsky, Z. & Stambler, N.) 119–150 (Springer, 2011).
7. Zoccola, D. *et al.* Bicarbonate transporters in corals point towards a key step in the evolution of cnidarian calcification. *Sci. Rep.* **5**, 9983 (2015).

8. Al-Horani, F. A., Al-Moghrabi, S. M. & de Beer, D. The mechanism of calcification and its relation to photosynthesis and respiration in the scleractinian coral *Galaxea fascicularis*. *Mar. Biol.* **142**, 419–426 (2003).
9. Venn, A. A. *et al.* Impact of seawater acidification on pH at the tissue-skeleton interface and calcification in reef corals. *Proc. Natl Acad. Sci. USA* **110**, 1634–1639 (2013).
10. Trotter, J. A. *et al.* Quantifying the pH 'vital effect' in the temperate zooxanthellate coral *Cladocora caespitosa*: validation of the boron seawater pH proxy. *Earth Planet. Sci. Lett.* **303**, 163–173 (2011).
11. Cohen, A. L. & McConnaughey, T. in *Biomineralization. Reviews in Mineralogy & Geochemistry*, Vol. 54 (eds Dove, P. M., Weiner, S. & Yoreo, J. J.) Ch. 6, 151–187 (The Mineralogical Society of America, 2003).
12. Yonge, C. M., Nicholls, A. G. & Yonge, M. J. in *Studies on the Physiology of Corals*, Vol. 1 (British Museum, 1931).
13. Goreau, T. Coral skeletal chemistry: physiological and environmental regulation of stable isotopes and trace metals in *Montastrea annularis*. *Proc. R. Soc. Lond. B Biol. Sci.* **196**, 291–315 (1977).
14. Allemand, D. *et al.* Biomineralisation in reef-building corals: from molecular mechanisms to environmental control. *C. R. Palevol.* **3**, 453–467 (2004).
15. Tambutté, S. *et al.* Coral biomineralization: from the gene to the environment. *J. Exp. Mar. Biol. Ecol.* **408**, 58–78 (2011).
16. Cai, W.-J. *et al.* Microelectrode characterization of coral daytime interior pH and carbonate chemistry. *Nat. Commun.* **7**, 11144 (2016).
17. McCulloch, M. T., Trotter, J. A., Falter, J. & Montagna, P. Coral resilience to ocean acidification and global warming through pH up-regulation. *Nat. Clim. Chang.* **2**, 623–627 (2012).
18. Holcomb, M. *et al.* Coral calcifying fluid pH dictates response to ocean acidification. *Sci. Rep.* **4**, 5207–5211 (2014).
19. Holcomb, M., DeCarlo, T. M., Gaetani, G. A. & McCulloch, M. Factors affecting B/Ca ratios in synthetic aragonite. *Chem. Geol.* **437**, 67–76 (2016).
20. Allison, N., Cohen, I., Finch, A. A., Erez, J. & Tudhope, A. W. Corals concentrate dissolved inorganic carbon to facilitate calcification. *Nat. Commun.* **5**, 5741 (2014).
21. Falter, J. L. *et al.* Assessing the drivers of spatial variation in thermal forcing across a nearshore reef system and implications for coral bleaching. *Limnol. Oceanogr.* **59**, 1241–1255 (2014).
22. Albright, R., Langdon, C. & Anthony, K. Dynamics of seawater carbonate chemistry, production, and calcification of a coral reef flat, central Great Barrier Reef. *Biogeosciences* **10**, 6747–6758 (2013).
23. McCulloch, M. T., Gagan, M. K., Mortimer, G. E., Chivas, A. R. & Isdale, P. J. A high-resolution Sr/Ca and $\delta^{18}\text{O}$ coral record from the Great Barrier Reef, Australia, and the 1982–1983 El Niño. *Geochim. Cosmochim. Acta* **58**, 2747–2754 (1994).
24. Falter, J. L., Lowe, R. J., Zhang, Z. L. & McCulloch, M. Physical and Biological controls on the carbonate chemistry of coral reef waters: effects of metabolism, wave forcing, sea level, and geomorphology. *PLoS ONE* **8**, e53303 (2013).
25. Takahashi, T. *et al.* Climatological distributions of pH, pCO₂, total CO₂, alkalinity, and CaCO₃ saturation in the global surface ocean, and temporal changes at selected locations. *Mar. Chem.* **164**, 95–125 (2014).
26. Holcomb, M., Cohen, A. L., Gabitov, R. I. & Hutter, J. L. Compositional and morphological features of aragonite precipitated experimentally from seawater and biogenically by corals. *Geochim. Cosmochim. Acta* **73**, 4166–4179 (2009).
27. Fine, M. & Tchernov, D. Scleractinian coral species survive and recover from decalcification. *Science* **315**, 1811 (2007).
28. Burton, E. A. & Walter, L. M. Relative precipitation rates of aragonite and Mg calcite from seawater: Temperature or carbonate ion control? *Geology* **15**, 111–114 (1987).
29. Erez, J., Reynaud, S., Silverman, J., Scheinder, K. & Allemand, D. in *Coral Reefs: an ecosystem in transition* (eds Dubinsky, Z. & Stambler, N.) 151–176 (Springer, 2011).
30. Georgiou, L. *et al.* pH homeostasis during coral calcification in a free ocean CO₂ enrichment (FOCE) experiment, Heron Island reef flat, Great Barrier Reef. *Proc. Natl Acad. Sci.* **112**, 13219–13224 (2015).
31. McCulloch, M. T. *et al.* Resilience of cold-water scleractinian corals to ocean acidification: Boron isotopic systematics of pH and saturation state up-regulation. *Geochim. Cosmochim. Acta* **87**, 21–34 (2012).
32. Chan, N. & Connolly, S. R. Sensitivity of coral calcification to ocean acidification: a meta-analysis. *Glob. Chang. Biol.* **19**, 282–290 (2013).
33. Gattuso, J. P. *et al.* Free-ocean CO₂ enrichment (FOCE) systems: present status and future developments. *Biogeosciences* **11**, 4057–4075 (2014).
34. Moya, A. *et al.* Carbonic anhydrase in the scleractinian coral *Stylophora pistillata* characterization, localization, and role in biomineralization. *J. Biol. Chem.* **283**, 25475–25484 (2008).
35. Tambutté, E. *et al.* Morphological plasticity of the coral skeleton under CO₂-driven seawater acidification. *Nat. Commun.* **6**, 7368 (2015).
36. Foster, T., Falter, J. L., McCulloch, M. T. & Clode, P. L. Ocean acidification causes structural deformities in juvenile coral skeletons. *Sci. Adv.* **2**, e1501130 (2016).
37. de Putron, S. J., McCorkle, D. C., Cohen, A. L. & Dillon, A. The impact of seawater saturation state and bicarbonate ion concentration on calcification by new recruits of two Atlantic corals. *Coral Reefs* **30**, 321–328 (2011).
38. Albright, R. & Langdon, C. Ocean acidification impacts multiple early life history processes of the Caribbean coral *Porites astreoides*. *Glob. Chang. Biol.* **17**, 2478–2487 (2011).
39. Randall, C. J. & Szmant, A. M. Elevated temperature affects development, survivorship, and settlement of the elkhorn coral, *Acropora palmata* (Lamarck 1816). *Biol. Bull.* **217**, 269–282 (2009).
40. Chua, C. M., Leggat, W., Moya, A. & Baird, A. H. Temperature affects the early life history stages of corals more than near future ocean acidification. *Mar. Ecol. Prog. Ser.* **475**, 85–92 (2013).
41. Alibert, C. & McCulloch, M. T. Strontium/calcium ratios in modern *Porites* corals from the Great Barrier Reef as a proxy for sea surface temperature: Calibration of the thermometer and monitoring of ENSO. *Paleoceanography* **12**, 345–363 (1997).
42. Reynolds, R. W. *et al.* Daily high-resolution-blended analyses for sea surface temperature. *J. Clim.* **20**, 5473–5496 (2007).
43. Chao, Y., Li, Z., Farrara, J. D. & Hung, P. Blending sea surface temperatures from multiple satellites and *in situ* observations for coastal oceans. *J. Atmos. Ocean. Technol.* **26**, 1415–1426 (2009).
44. Zhang, Z., Falter, J., Lowe, R. & Ivey, G. The combined influence of hydrodynamic forcing and calcification on the spatial distribution of alkalinity in a coral reef system. *J. Geophys. Res. Oceans* **117**, C04034 (2012).
45. Vengosh, A., Kolodny, Y., Starinsky, A., Chivas, A. R. & McCulloch, M. T. Coprecipitation and isotopic fractionation of boron in modern biogenic carbonates. *Geochim. Cosmochim. Acta* **55**, 2901–2910 (1991).
46. Mavromatis, V., Montouillout, V., Noireaux, J., Gaillardet, J. & Schott, J. Characterization of boron incorporation and speciation in calcite and aragonite from co-precipitation experiments under controlled pH, temperature and precipitation rate. *Geochim. Cosmochim. Acta* **150**, 299–313 (2015).
47. Hemming, N. G. & Hanson, G. N. Boron isotopic composition and concentration in modern marine carbonates. *Geochim. Cosmochim. Acta* **56**, 537–543 (1992).
48. Zeebe, R. & Wolf-Gladow, D. A. in *Elsevier Oceanography Series*, vol. 65 (Elsevier, 2001).
49. Foster, G. L., Pogge von Strandmann, P. A. E. & Rae, J. W. B. Boron and magnesium isotopic composition of seawater. *Geochem. Geophys. Geosyst.* **11**, Q08015 (2010).
50. Klochko, K., Kaufman, A. J., Yoa, W., Byrne, R. H. & Tossell, J. A. Experimental measurement of boron isotope fractionation in seawater. *Earth Planet. Sci. Lett.* **248**, 261–270 (2006).
51. Dickson, A. G. Thermodynamics of the dissociation of boric acid in synthetic seawater from 273.15 to 318.15 K. *Deep Sea Res. A* **37**, 755–766 (1990).
52. Sen, S., Stebbins, J. F., Hemming, N. G. & Ghosh, B. Coordination environments of B impurities in calcite and aragonite polymorphs: a ¹¹B MAS NMR study. *Am. Mineral.* **79**, 819–825 (1994).
53. Lewis, E. & Wallace, D. *Program Developed for CO₂ System Calculations* (Carbon Dioxide Information Analysis Center, Oak Ridge National Laboratory, U.S. Department of Energy, 1998).
54. Mehrbach, C., Culberson, C. H., Hawley, J. E. & Pytkowicz, R. N. Measurement of the apparent dissociation constants of carbonic acid in seawater at atmospheric pressure. *Limnol. Oceanogr.* **18**, 897–907 (1973).
55. Dickson, A. G. & Millero, F. J. A comparison of the equilibrium constants for the dissociation of carbonic acid in seawater media. *Deep Sea Res.* **34**, 1733–1743 (1987).
56. Dickson, A. G. Standard potential of the reaction: AgCl(s) + 1/2 H₂(g) = Ag(s) + HCl(aq) and the standard acidity constant of the ion HSO₄⁻ in synthetic seawater from 273.15 to 318.15 K. *J. Chem. Thermodyn.* **22**, 113–127 (1990).
57. Mucci, A. The solubility of calcite and aragonite in seawater at various salinities, temperatures, and one atmospheric total pressure. *Am. J. Sci.* **283**, 781–799 (1985).

Acknowledgements

This research was supported by funding provided from an ARC Laureate Fellowship (LF120100049) awarded to Professor Malcolm McCulloch and the ARC Centre of Excellence for Coral Reef Studies (CE140100020). Measurements of the $\delta^{11}\text{B}$ isotopic and B/Ca elemental ratios were conducted at the University of Western Australia's Advanced Geochemical Facility for Indian Ocean Research (AGFIOR), and we thank Anne-Marin Comeau and Dr Kai Rankenburg for their technical assistance.

Author contributions

M.T.M. wrote the draft of the manuscript and all authors (M.T.M., J.P.D., J.F., M.H. and J.A.T.) participated in collecting the geochemical data, analysing the results and shaping the final manuscript.

Additional information

Supplementary Information accompanies this paper at <http://www.nature.com/naturecommunications>

Competing interests: The authors declare no competing financial interests.

Reprints and permission information is available online at <http://npg.nature.com/reprintsandpermissions/>

How to cite this article: McCulloch, M. T. *et al.* Coral calcification in a changing World and the interactive dynamics of pH and DIC upregulation. *Nat. Commun.* **8**, 15686 doi: 10.1038/ncomms15686 (2017).

Publisher's note: Springer Nature remains neutral with regard to jurisdictional claims in published maps and institutional affiliations.



Open Access This article is licensed under a Creative Commons Attribution 4.0 International License, which permits use, sharing, adaptation, distribution and reproduction in any medium or format, as long as you give appropriate credit to the original author(s) and the source, provide a link to the Creative Commons license, and indicate if changes were made. The images or other third party material in this article are included in the article's Creative Commons license, unless indicated otherwise in a credit line to the material. If material is not included in the article's Creative Commons license and your intended use is not permitted by statutory regulation or exceeds the permitted use, you will need to obtain permission directly from the copyright holder. To view a copy of this license, visit <http://creativecommons.org/licenses/by/4.0/>

© The Author(s) 2017